21st Particles and Nuclei International Conference (PANIC 2017)
International Journal of Modern Physics: Conference Series
Vol. 46 (2018) 1860052 (7 pages)

DOI: 10.1142/S2010194518600522

Measurement of the Higgs Boson Mass in the $H \to ZZ^* \to 4\ell$ and $H \to \gamma\gamma$ Channels with $\sqrt{s} = 13\,\text{TeV}$ pp Collisions Using the ATLAS Detector

N. Bruscino (on behalf of the ATLAS Collaboration)
Department of Physics & Astronomy,
University of Pittsburgh, 4200 Fifth Avenue
Pittsburgh, PA 15260, USA
nello.bruscino@cern.ch

Published 3 May 2018

The mass of the Higgs boson is measured in the $H \to ZZ^* \to 4\ell$ and in the $H \to \gamma\gamma$ decay channels with $36.1\,\text{fb}^{-1}$ of proton-proton collision data from the Large Hadron Collider at a center-of-mass energy of $\sqrt{s} = 13$ TeV recorded by the ATLAS detector in 2015 and 2016. The measured value in the $H \to ZZ^* \to 4\ell$ channel is $m_H^{ZZ^*} = 124.88 \pm 0.37\,\text{GeV}$, while the measured value in the $H \to \gamma\gamma$ channel is $m_H^{\gamma\gamma} = 125.11 \pm 0.42\,\text{GeV}$. The two results have a compatibility of 0.4σ. The combined measurement from a simultaneous fit to the invariant mass distributions in the two channels is $m_H = 124.98 \pm 0.28\,\text{GeV}$.

Keywords: Higgs boson; mass; combination.

1. Introduction

The observation of a new particle in the search for the Standard Model (SM) Higgs boson H by the ATLAS and CMS experiments[1,2] with the LHC Run 1 data at center-of-mass energies of $\sqrt{s} = 7\,\text{TeV}$ and $8\,\text{TeV}$ has been a major step towards understanding the mechanism of electroweak (EW) symmetry breaking. Its mass has been measured with a simultaneous fit to the ATLAS and CMS Run 1 data to be 125.09 ± 0.24 GeV[3].

The measurement of the mass of the Higgs boson in Run 2[4] is performed with $36.1\,\text{fb}^{-1}$ of pp collision data recorded with the ATLAS detector at a center-of-mass energy of $\sqrt{s} = 13$ TeV: it is derived from a combined fit to the invariant mass spectra of the decay channels $H \to ZZ^* \to 4\ell$ ($\ell = e, \mu$) and $H \to \gamma\gamma$, based on the current understanding of the reconstruction, identification, and calibration of muons, electrons, and photons in the ATLAS detector[5].

2. Physics object reconstruction

Since the two analyses make use of several leptons and photons in the final state, their reconstruction and calibration are crucial aspects for the best measurement.

Muons are reconstructed combining tracks from the inner detector (ID) and the muon spectrometer (MS), according to various algorithms based on the information provided by the ID, the MS and the calorimeters. Although the simulation accurately describes the ATLAS detector, additional corrections to the simulated momentum are needed in order to match the simulation to data precisely. The muon momentum resolution and momentum scale are parametrised as a power expansion in the muon p_{T}, as a function of η and ϕ, from large samples of $J/\psi \to \mu^+\mu^-$ and $Z \to \mu^+\mu^-$ decays. The local misalignments of the ID in 2016 bias the muon track sagitta and result in a charge-dependent bias ($\mathcal{O}(1\,\mathrm{TeV}^{-1})$) of the reconstructed muon momentum, which is studied and corrected in data by comparing the local inhomogeneities of the charge dependent dimuon mass to the mass of well-known neutral resonances.

Photon and electron candidates are reconstructed from clusters of energy deposited in the electromagnetic calorimeter with and without a matching track or reconstructed conversion vertex in the ID. The energy measurement is performed by summing the energies measured in the EM calorimeter cells belonging to the candidate cluster. The cluster energy is corrected for energy loss in the inactive materials or deposited outside the area of the cluster and for the amount of energy deposited into the hadronic calorimeter. The calibration coefficients are obtained from a detailed simulation of the detector response to electrons and photons, and are optimised with a boosted decision tree (BDT). The response is calibrated separately for electrons, converted and unconverted photon candidates. Moreover, a global calorimeter energy scale correction, determined in situ with a large sample of $Z \to e^+e^-$ events and verified using $J/\psi \to e^+e^-$ and $Z \to \ell^+\ell^-\gamma$ events, is applied.

3. Mass measurement in the $H \to ZZ^* \to 4\ell$ channel

Events are required to contain four isolated charged leptons ($\ell = e, \mu$), grouped into two pairs of oppositely charged leptons of the same flavour and that emerge from a common vertex. The first three leptons have p_{T} larger than 20, 15 and 10 GeV, respectively; the forth muon (electron) is required to pass a 5 (7) GeV cut. The lepton pair with an invariant mass closest to the Z boson pole mass is referred to as the leading dilepton pair. The selected events are split according to the flavour of the leading and subleading pairs (4μ, $2e2\mu$, $2\mu 2e$, $4e$). Using the corrected value of $m_{4\ell}$, events with $110 < m_{4\ell} < 135\,\mathrm{GeV}$ are used for the Higgs boson mass measurement. The selected events have a small contribution from reducible background processes: Z+jets, $t\bar{t}$, and WZ production which are selected if at least one of the jets in the final states is misidentified as a prompt isolated lepton. Non-resonant ZZ^* production with a final state topology similar to the $H \to ZZ^* \to 4\ell$ signal is the main background contribution and is modelled using simulation normalised to the SM prediction.

Since the Higgs boson is more centrally produced than the non-resonant ZZ^* production and tends to have larger transverse momentum, the transverse momentum and pseudorapidity of the four-lepton system are used together with a matrix-element-based kinematic discriminant $D_{ZZ^*} = \ln(|\mathcal{M}_{HZZ^*}|^2/|\mathcal{M}_{ZZ^*}|^2)$ as inputs to a boosted decision tree (BDT) to discriminate the $H \to ZZ^* \to 4\ell$ signal from the $ZZ^* \to 4\ell$ background. The events are categorised in four exclusive equal-size BDT bins in order to better separate the signal from the background contribution in the m_H fit. The separation of signal from background brought by the BDT output brings 6% improvement on m_H resolution in the 4ℓ decay channel.

The mass of the Higgs boson is determined from the position of the peak in the four-lepton invariant mass distribution around 125 GeV. This distribution is a superposition of a signal distribution S_{m_H}, which is a function of the mass of the Higgs boson m_H, and a background distribution B, which is independent of m_H. Templates from simulation are used to model the background distribution B in the fit. The shape of the signal distribution depends on the four-lepton invariant mass resolution which varies event by event. This variation is taken into account by the so-called "per-event method".

3.1. *Per-event method*

The measured $m_{4\ell}$ signal distribution is modelled as the convolution of the intrinsic Higgs boson lineshape, assumed to be a relativistic Breit-Wigner (BW) distribution with width equal to the SM value and mass m_H free in the fit, with a four-lepton invariant mass response function F, which gives the probability of measuring a value $m_{4\ell}^{\mathrm{meas}}$ for a true invariant mass $m_{4\ell}^{\mathrm{true}}$:

$$S_{m_H}(m_{4\ell}^{\mathrm{meas}}) = \int_0^\infty F(m_{4\ell}^{\mathrm{meas}} - m_{4\ell}^{\mathrm{true}}) \cdot BW(m_{4\ell}^{\mathrm{true}}, m_H)\, dm_{4\ell}^{\mathrm{true}}. \tag{1}$$

The response function is derived using simulation from the lepton energy response functions which describe the probability of measuring a lepton energy E^{meas} given its true energy E^{true}. The lepton energy response functions can be parametrised by a linear superposition of three normal distributions, obtained separately for electrons and muons and depending on both the lepton energy and the detector region in which the lepton energy is measured. The four-lepton invariant mass response function is therefore a convolution of $3^4 = 81$ normal distributions and varies from one event to another. To simplify the probability density function (p.d.f.), the number of normal distributions can be reduced by following an iterative procedure. As the uncertainty on the mass measurement depends linearly on the resolution, the $m_{4\ell}$ resolution is improved by constraining the mass of the leading lepton pair to the lineshape of the Z boson. This allows about 15% improvement in the four-lepton mass resolution.

Finally, the mass of the Higgs boson m_H is determined by maximising the likelihood function $L(m_H) = \prod_{k=1}^{N} \left[S^{(k)}_{m_H} \left(m_{4\ell}^{\text{meas(k)}} \right) + B \left(m_{4\ell}^{\text{meas(k)}} \right) \right]$ as a function of m_H, where the index k denotes the k^{th} event and N the number of selected events and B the p.d.f. for the background.

3.2. *Results*

The estimate of m_H is extracted with a simultaneous profile likelihood fit to the sixteen categories (one for each final state and for each BDT bin) of data. The observed total uncertainty in m_H is of ± 0.37 GeV. Using an alternative method it is found to be $^{+0.41}_{-0.40}$ GeV, larger by about 35 MeV than for the per-event method. Figure 1 shows the addition of the projections of the fits to the different categories compared to the combined 4ℓ data.

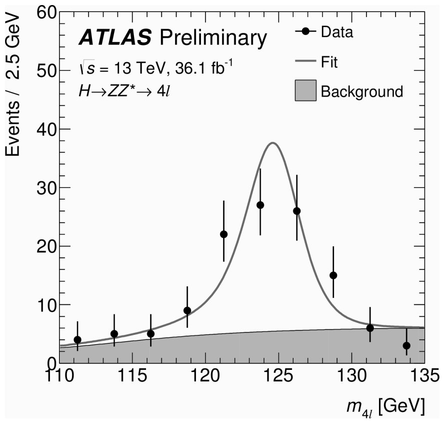

Fig. 1. Invariant mass distribution of the data (points with error bars) shown together with the projection of the simultaneous fit result to $H \to ZZ^* \to 4\ell$ candidates (continuous line). The background component of the fit is also shown (filled area). The signal p.d.f. is evaluated per-event and averaged over the observed data.

The measured value of m_H is found to be $m_H^{ZZ^*} = 124.88 \pm 0.37$ (stat) $\pm$ 0.05 (syst) GeV$= 124.88 \pm 0.37$ GeV. The total uncertainty is in agreement with the expectation of ± 0.35 GeV and is dominated by the statistical component. The total systematic uncertainty is 47 MeV, with the leading sources being the muon momentum scale (40 MeV), the electron energy scale (20 MeV), the background modelling (10 MeV) and the simulation statistics (8 MeV).

4. Mass measurement in the $H \to \gamma\gamma$ channel

A first preselection is applied requiring at least two reconstructed photons with $E_{\mathrm{T}} > 25$ GeV and $|\eta| < 2.37$, excluding the region $1.37 \leq |\eta| \leq 1.52$. Photons are required to pass loose identification criteria. The two reconstructed photon candidates with the largest E_{T} are considered and used to identify the diphoton primary vertex. Selecting the correct diphoton vertex is important to keep the contribution of the opening angle resolution to the diphoton mass resolution significantly smaller than the energy resolution contribution. Thus, a neural network algorithm, which combines information from the tracks and primary vertices, is employed. The two photons are required to have $E_{\mathrm{T}}/m_{\gamma\gamma} > 0.35$ and 0.25 respectively, and to pass the tight identification criteria and isolation criteria. Only events with $105\,\mathrm{GeV} \leq m_{\gamma\gamma} \leq 160\,\mathrm{GeV}$ are kept. The properties of the two selected photons and of the additional selected objects (b-jets, leptons, ...) are used to categorize the events in 31 mutually exclusive categories.

4.1. *Signal models*

For each category the shape of the diphoton invariant mass distribution is modelled with a double-sided Crystal Ball function, *i.e.* a Gaussian function in the peak region with power-law functions in both tails:

$$f(m_{\gamma\gamma}) = \begin{cases} e^{-t^2/2} & \text{if } -\alpha_{\mathrm{low}} \leq t \leq \alpha_{\mathrm{high}} \\ \dfrac{e^{-\frac{1}{2}\alpha_{\mathrm{low}}^2}}{\left[\frac{1}{R_{\mathrm{low}}}(R_{\mathrm{low}}-\alpha_{\mathrm{low}}-t)\right]^{n_{\mathrm{low}}}} & \text{if } t < -\alpha_{\mathrm{low}} \\ \dfrac{e^{-\frac{1}{2}\alpha_{\mathrm{high}}^2}}{\left[\frac{1}{R_{\mathrm{high}}}(R_{\mathrm{high}}-\alpha_{\mathrm{high}}+t)\right]^{n_{\mathrm{high}}}} & \text{if } t > \alpha_{\mathrm{high}} \end{cases}$$

where $t = (m_{\gamma\gamma} - \mu_{\mathrm{CB}})/\sigma_{\mathrm{CB}}$, $R_{\mathrm{low}} = \frac{n_{\mathrm{low}}}{\alpha_{\mathrm{low}}}$, and $R_{\mathrm{high}} = \frac{n_{\mathrm{high}}}{\alpha_{\mathrm{high}}}$. μ_{CB} and σ_{CB} represent the position of the peak and the width of the Gaussian distribution, while α_{low}, α_{high}, n_{low} and n_{high} are parameters related to the tails.

4.2. *Background models*

In each category, the invariant mass distribution of the sum of all background processes is parameterized with a continuous function: the parameters and normalizations are fitted directly on data. The functional form used in each category is chosen as the one that minimizes the fitted signal yield on a sample of background only events. This background only sample is built from events selected from control regions or from simulations depending on the background process. An F-test is performed on data-sidebands to check whether functions with extra degrees of freedom describe the data significantly better. The procedure selects simple exponential distributions for the categories with less events while power-law functions or exponential functions of a second-order polynomial are used for the others.

4.3. *Results*

The Higgs boson mass in the diphoton channel $m_H^{\gamma\gamma}$ is estimated with a binned maximum likelihood fit, considering the data in all the categories simultaneously. The parameters of the fit are $m_H^{\gamma\gamma}$, the four signal strengths, the number of background events, the parameters describing the shape of the background invariant mass distribution and all the nuisance parameters associated to systematic uncertainties.

Figure 2 shows the distribution of the data superimposed with the result of the simultaneous fit; for illustration purposes events in each category are weighted by the corresponding factor $\ln(1 + s_{90}/b_{90})$.

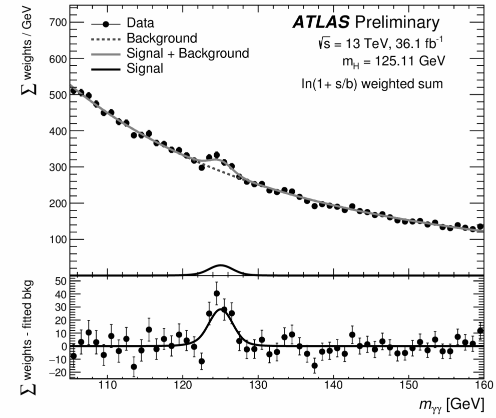

Fig. 2. Diphoton invariant mass distribution of the data superimposed with the result of the fit. The dashed line represents the background component of the model, while the black line the signal component. The bottom inset is the difference between the sum of weights and the background component of the fitted model.

The measured mass of the Higgs boson in the diphoton channel is $m_H^{\gamma\gamma} = 125.11 \pm 0.21\,(\text{stat}) \pm 0.36\,(\text{syst})\,\text{GeV} = 125.11 \pm 0.42\,\text{GeV}$, where the total systematic uncertainty is dominated by the photon energy scale uncertainty.

5. Combined mass measurement

The Higgs boson mass is measured combining information from both the $H \to ZZ^* \to 4\ell$ and $H \to \gamma\gamma$ channels. Different m_H values are tested using a profile likelihood ratio defined in terms of m_H, while treating the signal strengths (μ^{ZZ}, $\mu^{\gamma\gamma}_{\text{ggH}}$, $\mu^{\gamma\gamma}_{\text{VBF}}$, $\mu^{\gamma\gamma}_{\text{VH}}$, $\mu^{\gamma\gamma}_{\text{ttH}}$) as independent nuisance parameters. The main sources of correlated systematic uncertainty include the calibrations of electrons, photons, the pileup modelling, and the luminosity.

The combined mass measured is

$$m_H = 124.98 \pm 0.19\ (\text{stat}) \pm 0.21\ (\text{syst})\,\text{GeV} = 124.98 \pm 0.28\,\text{GeV},$$

where the first (second) uncertainty corresponds to the statistical (systematic) component. The main sources of systematic uncertainty on the combined mass measurement are the photon and electron energy scale uncertainties.

The combined mass measured is in excellent agreement with, and has similar precision to, the value that was measured with a combined fit to the ATLAS and CMS Run 1 data, $m_H = 125.09 \pm 0.21\ (\text{stat}) \pm 0.11\ (\text{syst})\,\text{GeV} = 125.09 \pm 0.24\,\text{GeV}$.

References

1. ATLAS Collaboration, *Phys. Lett. B* **716** 1 (2012).
2. CMS Collaboration, *Phys. Lett. B* **716** 30 (2012).
3. ATLAS Collaboration, *Phys. Rev. Lett.* **114** 191803 (2015).
4. ATLAS Collaboration, CONF-2017-046 *2017 EPS Conference* (2017).
5. ATLAS Collaboration, *JINST* **3** S08003 (2008).